

## Structure and Piezoelectricity of Poly(vinylidene fluoride) Films Obtained by Solid-State Extrusion

Shigeru TASAKA, Jun NIKI, Takeaki OJIO,  
and Seizo MIYATA

*Material Systems Engineering, Faculty of Technology,  
Tokyo University of Agriculture and Technology,  
Nakamachi, Koganei, Tokyo 184, Japan*

(Received September 27, 1983)

**ABSTRACT:** Solid-state extrusion of poly(vinylidene fluoride) and its coextrusion with polyethylene were carried out using a slit die (die angle = 35°) at 400 MPa. Extrudates with smooth surfaces were obtained at extrusion ratios from 2.0 to 6.5. Wide-angle X-ray diffractions of the extrudates showed double orientation characteristic of the form I crystals, with the *c*-axis preferentially oriented in the machine direction and the *b*-axis parallel to the film surface. The piezoelectric constant  $d_{31}$  of the extrudates increased with increasing extrusion ratio, but decreased with increasing extrusion temperature. Thus, the piezoelectric activity may be explained by changes in Poisson's ratio and Young's modulus, perfection of crystallites, and selective orientation.

**KEY WORDS** Solid-State Extrusion / Poly(vinylidene fluoride) / Orientation / Piezoelectricity /

Physical properties of semicrystalline polymers depend not only on chemical structure but also on superstructure such as crystal orientation and the combination of crystal and amorphous regions. For example, fibers prepared by zone-drawing<sup>1</sup> and high pressure extrusion<sup>2-8</sup> show both high modulus and strength due to the alignment of the fiber axis. In particular, the high pressure extrusion technique for enhancing various physical properties has received increasing attention in recent years. An attempt has been made to extrude a solid state polymer into a fibrous or film shape in order to obtain high mechanical and thermal properties as well as better transparency.

Solid-state extrusion, which can be controlled by temperature, pressure, time and deformation mode, makes possible the production of polymers with new superstructures. Therefore, many crystalline polymers such as linear polyethylene,<sup>2</sup> polypropylene,<sup>3</sup> poly-1-butene,<sup>4,5</sup> nylons<sup>6</sup> and poly(vinylidene fluoride)<sup>7,8</sup> have been extruded in the solid state by

various methods. Among these polymers, poly(vinylidene fluoride) (PVDF) is now attracting attention not only because of the complexity of its crystal structure but also because of its possible use as a transducer. The solid-state extrusion of PVDF was first carried out by Kolbeck *et al.*<sup>3</sup>; however, they were unable to obtain a continuous extrudate. But following that, Shimada *et al.*<sup>8</sup> succeeded in doing so by coextrusion with polyethylene, and reported high birefringence. However, the relationship between the structure and electric properties has not yet been clarified.

PVDF exists in the four crystal forms designated as I, II, polar II and III. Form I PVDF exhibits structure sensitive piezo, pyro and ferroelectric behavior. The piezoelectric activity is enhanced by stretching<sup>9</sup> or rolling<sup>10</sup> PVDF films prior to poling. Solid-state extrusion is more effective than other methods for improving the molecular chain orientation. A large piezoelectric activity may be obtained by controlling the molecular orientation by

extrusion.

The present paper describes the structure and piezoelectricity of poly(vinylidene fluoride) obtained by solid-state film extrusion. Further, the effects of molecular orientation on the physical properties of PVDF are discussed.

## EXPERIMENTAL

The PVDF sample (KF#1100) used in this study was manufactured by Kureha Chemical Industry Co., Ltd. The extrusion apparatus, with the pulling mechanism for applying a stress to the extrudate in the die head, was similar to the apparatus employed previously for the solid state extrusion of polymers.<sup>5</sup> The film extrusion was performed by inserting a PVDF flat billet into a film extrusion die placed in a high pressure vessel. The slit die consisted of identical half-dies matched along a vertical plane in the pressure vessel. Each half-die had three zones, the initial, tapered and untapered zones, as reported previously.<sup>5</sup> A die angle of 35°, which is given in terms of the space angle of the conically tapered dies, was employed in this study. Lead was used both as a pressure medium and pressure sealant. The extrusion ratio  $R$  is defined by the ratio ( $A_0/A$ ), where  $A_0$  is the original cross sectional area and  $A$ , that of the extrudate. The ram extrusion with lead<sup>5</sup> was performed when the extrusion ratio was not very large ( $R=1-4$ ). For high extrusion ratios ( $R=4-7$ ), coextrusion with polyethylene using the method of Shimada *et al.*<sup>8</sup> was employed (Figure 1). Both extrusions were carried out between 50 and 170°C at 400 MPa. The dimensions of the extrudate for the film extrusion were 1.2 cm in width and 0.005–0.05 cm in thickness.

Wide angle X-ray diffractions were obtained by nickel-filtered Cu-K $\alpha$  radiation with a micro-Laue-camera, and a flat plate camera. The piezoelectric constant, dielectric constant and Young's modulus were measured with apparatus similar to that developed by

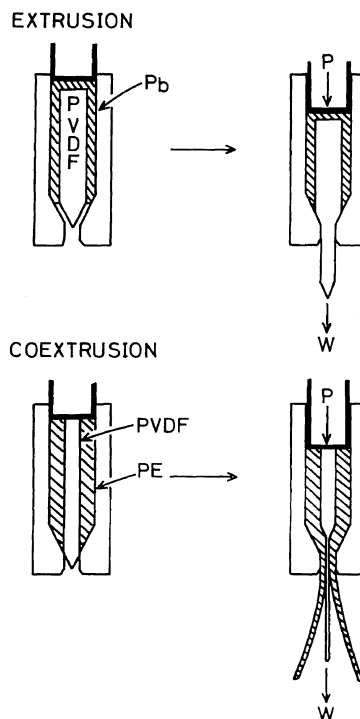


Figure 1. Schematic representation of extrusion and coextrusion.

Furukawa *et al.*<sup>11</sup> The poling conditions were  $T_p = 120^\circ\text{C}$ ,  $E_p = 20 \text{ MV/m}$ , and  $t_p = 1 \text{ h}$ .

## RESULTS AND DISCUSSION

### (1) Extrusion Behavior

Both continuous and discontinuous extrusions were observed in a ram extrusion. The continuous extrudates were obtained at temperatures above 100°C and low extrusion ratios ( $R=1.5-3.8$ ). On the other hand, discontinuous extrusion with fractured deformation was observed at high extrusion ratios and temperatures below 100°C. Therefore, it was virtually impossible to obtain highly oriented continuous extrudates by the ram method. Consequently, higher extrusion ratios ( $R=4-6.5$ ) were obtained by coextrusion with high density polyethylene, as was done successfully by Shimada *et al.*<sup>8</sup> In our case, the deforma-

tion style was not simple elongation, but the width of the films was kept constant. All successful extrudates, obtained by applying a 14 MPa load at the end of the extrudate during the extrusion, had smooth surfaces and transparency. The extrusion rate ranged from 0.5 to 2 mm/min, depending on the extrusion ratio and temperature.

## (2) Structure of Extrudates

Figure 2 shows X-ray micro-photographs at

various stages (a—h) of the extrusion in which the structure of PVDF was transformed from form II to form I as extrusion proceeded. At the first stage, the extrudate showed specific orientation so that the diffraction by the (020) and (110) planes of the form II crystal could be observed along the line inclining at about  $25^\circ$  from the meridian line (photographs (b) and (c)). These diffraction patterns appeared when the *c*-axis of the form II crystal tilted  $25^\circ$  away from the mechanical direction. The tilting

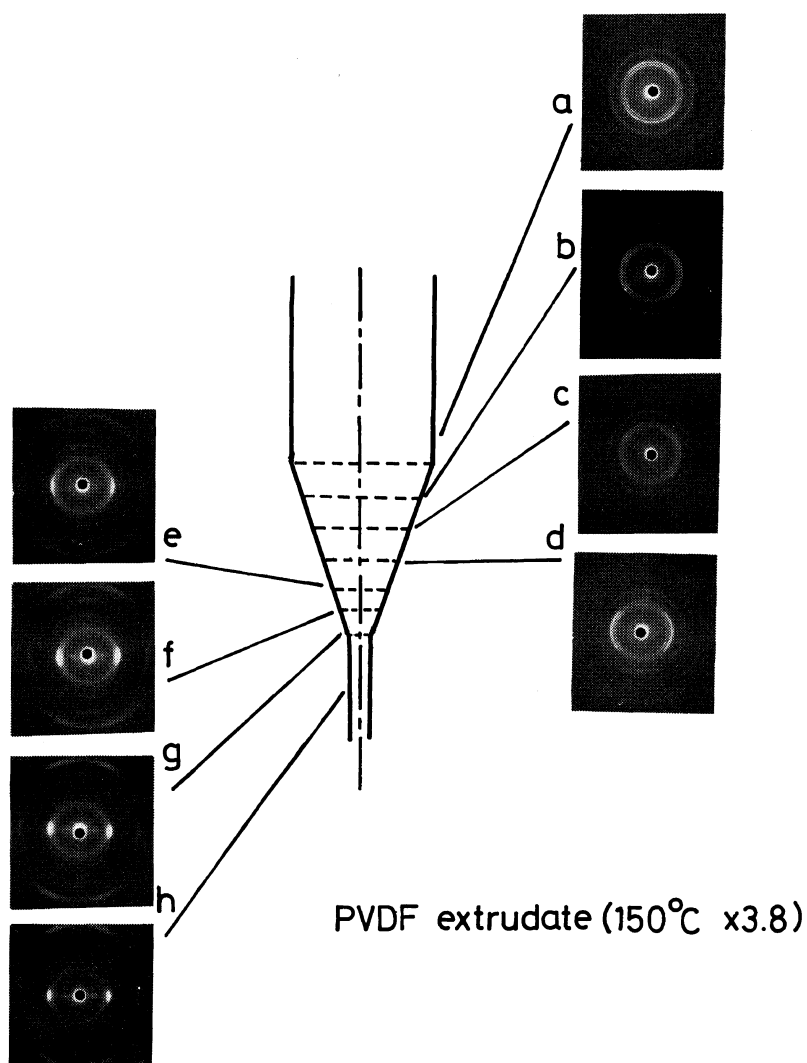
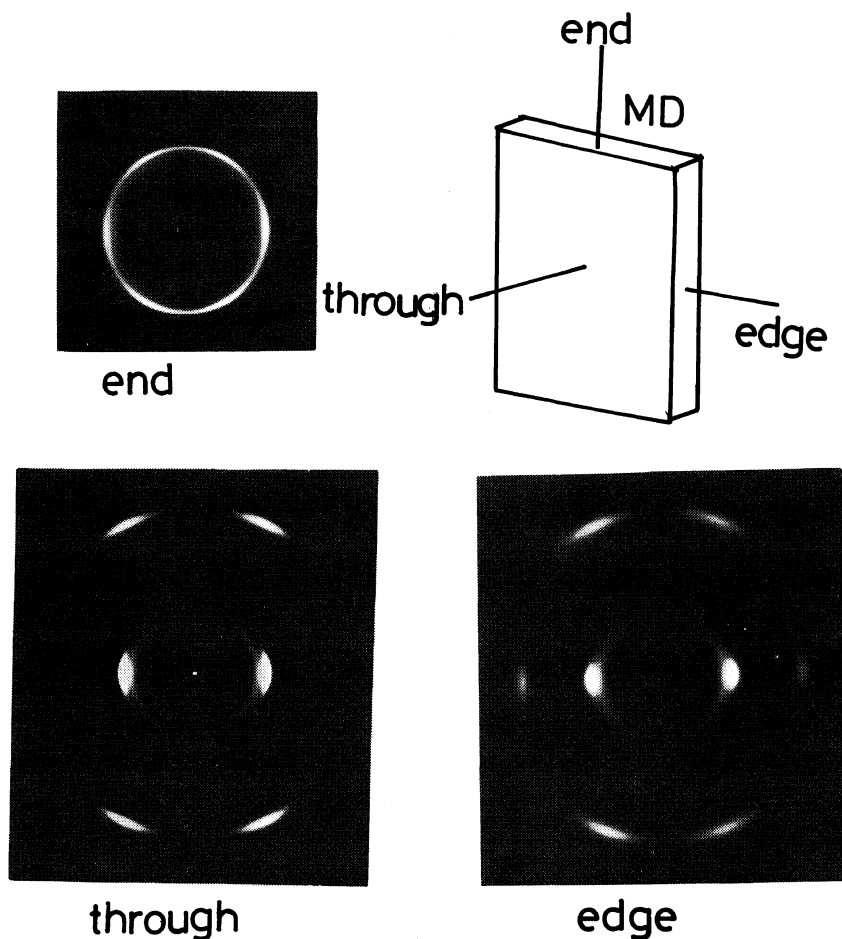


Figure 2. Wide-angle X-ray diffraction patterns in the process of a ram extrusion of PVDF.

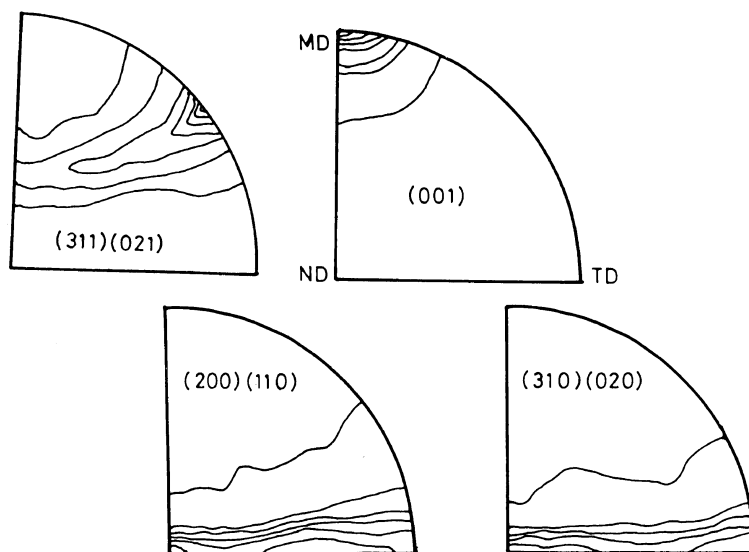
was caused by shear deformation resulting from high pressure extrusion. Further, diffraction spots caused by the (021) and (110) planes could be seen in the equatorial and meridian lines, respectively (photograph (d)). This behavior is related to the orientation of a specific plane, but cannot be explained simply. During the middle extrusion stages the tilted form II crystal was transformed into the oriented form I crystal (photograph (e)). During the (f)–(h) stages, a highly oriented film is formed.

Figure 3 shows wide angle X-ray photographs of the extrudates of the 4.8 extrusion

ratio at 100°C, taken from three directions (through, edge and end). These show no diffraction spots due to form II. From the through photograph, it may be considered that the fibers are oriented parallel to the extrusion direction as was observed in the fibrous extrusion. But some differences could be seen between the spot from the through and that from the edge direction, indicating double orientation instead of simple uniaxial orientation. However, it was difficult to determine the characteristic structure associated with this orientation, since the form I crystal of PVDF had an orthorhombic structure which was



**Figure 3.** Wide-angle X-ray diffraction patterns for an extrudate of PVDF. ( $R=4.8$ , coextrusion with PE)



PVDF extrudate (150°C, x 3.8)

Figure 4. Pole figures for an extrudate of PVDF.

hardly distinguished from the pseudohexagonal, so that the diffractions from some different planes were observed as a single Bragg diffraction.

Here, we suggest two possible orientations on the basis of the end photograph: the  $a$ -axis is oriented normal to the film surface or the  $a$ -axis is oriented with an inclination of 60° or 120° to the film surface, implying that the (110) plane aligns preferentially perpendicular to the film surface. The determination of this can be made by pole-figure analysis.

Figure 4 shows the pole figures for an extrudate (100°C,  $R=4.8$ ) taken from three directions. Here, MD defines the extrusion direction, ND, the thickness direction and TD, the transverse direction. The pole of the (001) reflection shows a high degree of orientation of the  $c$ -axis. The (310,020) pole distributes normal to MD, and has two maxima. This figure can be explained by either of the above assumptions. However, basic information can be obtained on the  $b$ -axis from the (311,021) pole, since the (021) diffraction intensity is

about three times that of the (311), according to calculations of Takahashi *et al.*<sup>12</sup> The maximum position of the (311,021) pole figure, which is at a polar angle of 46°, suggests that the  $b$ -axis aligns parallel to the film surface.

In summary, most extrudates show double orientation in which the  $c$ -axis is preferentially oriented in the extrusion direction and the  $b$ -axis is parallel to the film surface.

Figure 5 shows small angle X-ray scattering (SAXS) photographs in two directions (through and edge) for extrudates prepared at various extrusion temperatures. Four point diagrams can be seen in the edge views in the temperature range employed while a change from a four point clover form to a two point one can be seen in the through view. Further, the vertical angle of the quadrant diagram in the edge view is constant at all temperatures. The differences in the vertical angle between the edge and through views result from anisotropic shear deformation in the slit die. The long periods calculated from Figure 5 are 110 Å (50°C), 130 Å (100°C), and 180 Å (150°C).

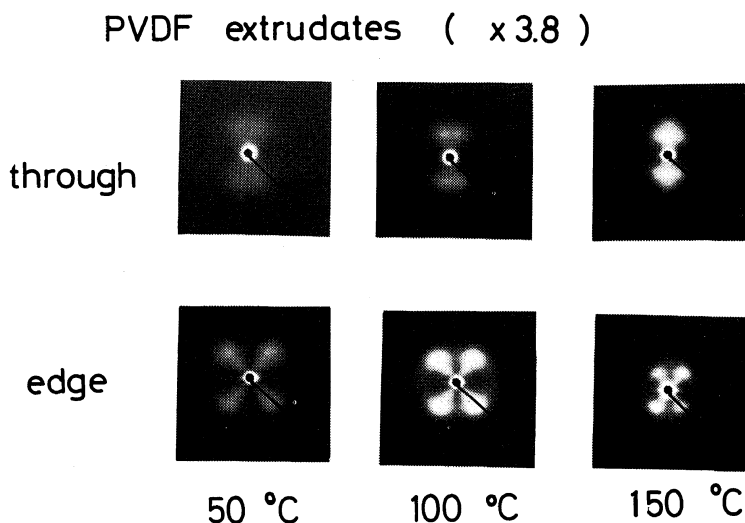


Figure 5. Changes in small-angle X-ray scattering for an extrudate with extrusion temperature.

This change in the long period with temperature can be explained as resulting from annealing, since the same change may be caused by annealing only.

### (3) Electrical Properties of Extrudates

Figure 6 shows plots of the dielectric constant  $\epsilon_3$ , the piezoelectric constant  $d_{31}$  and Young's modulus  $c_{11}$  against the draw ratio  $R$  for extrudates at room temperature. The dielectric constant and Young's modulus increase with  $R$ , because of the increasing orientation of the molecular chain in the amorphous and crystalline regions. The degree of  $c$ -axis orientation was calculated as 0.97 by the X-ray method going on the assumption of a simple uniaxial orientation when  $R$  is larger than 3. The birefringence ( $\Delta n$ ) of the extrudates, measured using a polarizing microscope, also showed a very high value of 0.047 at  $R=6.5$ . This large birefringence is related to enhancement of the amorphous orientation and selective orientation in the crystallites. Further, the difference in birefringence between the through ( $\Delta n_t$ ) and the edge ( $\Delta n_e$ ) directions is expressed as  $\Delta n_t - \Delta n_e = 0.005 - 0.01$  ( $R=4$ ), which is a measure of double orientation simi-

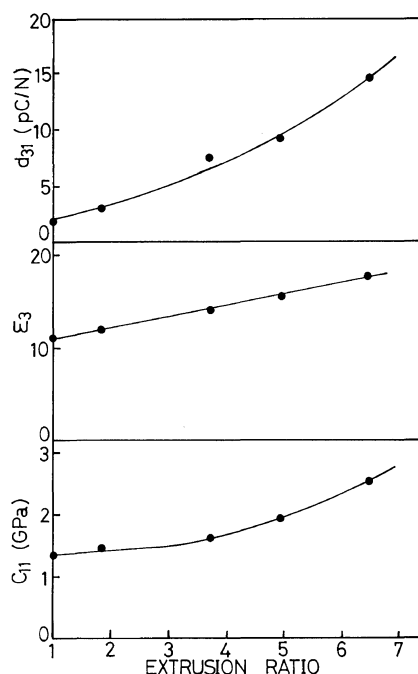


Figure 6. Plots of piezoelectric constant  $d_{31}$ , dielectric constant  $\epsilon_3$  and Young's modulus  $c_{11}$  against extrusion ratio.

lar to that obtained from X-ray results. The piezoelectric constant is likely to increase with increasing extrusion ratio, since high ex-

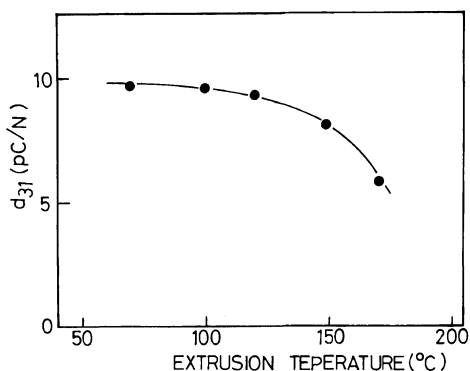


Figure 7. Extrusion temperature dependence of piezoelectric constant  $d_{31}$  for the coextrudates ( $R=3.8$ ) poled at  $120^\circ\text{C}$ . ( $E_p=20\text{ MV/m}$ )

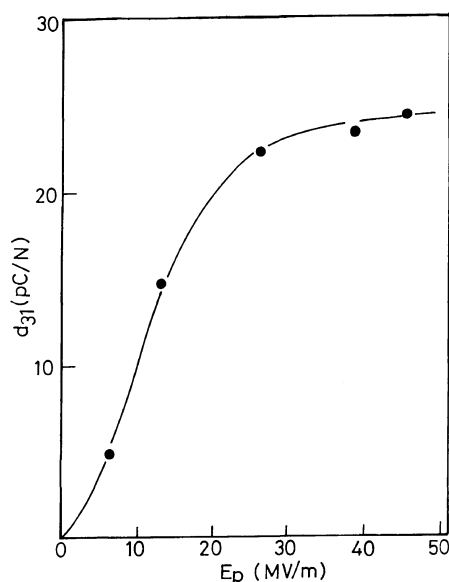


Figure 8. Poling electric field dependence of piezoelectric constant  $d_{31}$ , for the coextrudates ( $R=4.6$ ) poled at  $120^\circ\text{C}$ .

trusion ratio leads to an increase in the form I crystal fraction, the Poisson's ratio and the electrostrictive constant as already proposed.<sup>13</sup>

Figure 7 shows the extrusion temperature dependence of the piezoelectric constant  $d_{31}$  ( $R=3.8$ ). The piezoelectricity decreased gradually with a rise in extrusion temperature.

Table I. Comparison of the physical properties of a extrudate and an undrawn film

	Coextrudate ( $100^\circ\text{C} \times 4.6$ )	Undrawn (melt cast)
$\mu_{31}$	0.85	0.33
$c_{11}$ (GPa)	1.90	1.63
$\Delta n (\times 10^{-3})$	46.1	—
$\epsilon_3$	14.6	11.4
$d_{31}$ (pC/N)	23.8	2.0
$d_{33}$ (pC/N)	-29	-5
$\kappa_{31}$	10.2	-0.67

$\mu_{31}$ , Poisson's ratio;  $d_{31}$ , piezoelectric constant;  $c_{11}$ , Young's modulus;  $d_{33}$ , piezoelectric constant;  $\Delta n$ , birefringence;  $\kappa_{31}$ , electrostriction constant;  $\epsilon_3$ , dielectric constant.

This behavior may arise from one of the following two facts. First, Poisson's ratio and the electrostriction constant of extrudate obtained at high temperature are smaller than those obtained at low temperature. The annealing at high temperature causes decrease in amorphous orientation which is related to these two factors.<sup>14</sup> Second, the residual polarization induced by poling decreases because of the difficulty of dipole rotation in the crystals which are stabilized and thickened by annealing as reported previously.<sup>15</sup>

Figure 8 shows the relationship between the poling field and the piezoelectric constant for specimens extruded 4.6 times their original length at  $100^\circ\text{C}$ . In comparison with an ordinary uniaxially drawn film, the piezoelectric constant of the extrudate appeared to become saturated at a low poling field, but the saturation value was not very large. This behavior may arise from the orientation of the  $b$ -axis, in which the CF dipoles align parallel to the plane of the film. The saturation at the low field indicates a low coercive field of the extrudate.

If the dipoles rotate about the direction of the electric field at steps of  $60^\circ$  as proposed by Kepler *et al.*,<sup>16</sup> most of them cannot orient normal to the film surface of the extrudate.

When the isotropic dipole orientation changes to the polar distribution, the polarization is limited to 86% of that of the perfectly oriented state. However, this effect does not contribute particularly to the piezoelectric constant. The effect of the internal field applied to oriented crystallites should be taken into account for the saturation in Figure 8.

The electrical properties of the extrudate and the original form II films are compared in Table I. The extrudate has a large Poisson's ratio, birefringence and piezoelectric constants,  $d_{31}$  and  $d_{33}$ . Poisson's ratio, which depends on anisotropic lamella structures,<sup>13</sup> is related to the structure, as expected from the small angle X-ray scattering shown in Figure 5. Only the electrostrictive constant is smaller than that of the uniaxially drawn sample.<sup>17</sup> This fact may be explained by the decrease in amorphous orientation of the extrudate due to high extrusion temperature. It may be expected that high extrusion ratios (more than  $R=10$ ) obtained by the coextrusion method yield a large electrostriction constant and piezoelectric constant.

In conclusion, the solid-state extrusion of PVDF was achieved by the method of coextrusion with polyethylene. It was found that the extrudate has a special structure characteristic of piezoelectric polymers.

*Acknowledgement.* This work was support-

ed in part a Grant-in-Aid from the Ministry of Education in Japan.

## REFERENCES

1. K. Kamezawa, Y. Yamada, and M. Takayanagi, *J. Appl. Polym. Sci.*, **24**, 1227 (1979).
2. C. R. Desper, J. H. Southern, R. D. Uhlrich, and R. S. Porter, *J. Appl. Phys.*, **41**, 4285 (1970).
3. A. G. Kolbeck and D. R. Uhlmann, *J. Polym. Sci., Polym. Phys. Ed.*, **15**, 27 (1977).
4. R. Ball and R. S. Porter, *J. Polym. Sci., Polym. Lett.*, **15**, 519 (1977).
5. S. Tasaka, T. Suzuki, and S. Miyata, *Kobunshi Ronbunshu*, **39**, 127 (1982).
6. W. G. Perkins and R. S. Porter, *Bull. Am. Phys. Soc.*, **AJ10**, 235 (1976).
7. W. T. Mead, A. E. Zachariades, T. Shimada, and R. S. Porter, *Macromolecules*, **12**, 473 (1979).
8. T. Shimada, A. E. Zachariades, W. T. Mead, and R. S. Porter, *J. Crystal Growth*, **48**, 334 (1980).
9. H. Kawai, *Jpn. J. Appl. Phys.*, **8**, 975 (1969).
10. T. T. Wang, *J. Appl. Phys.*, **50**, 6091 (1979).
11. T. Furukawa and E. Fukada, *J. Polym. Sci., Polym. Phys. Ed.*, **14**, 1979 (1976).
12. N. Takahashi and A. Odajima, *Ferroelectrics*, **32**, 49 (1981).
13. S. Tasaka and S. Miyata, *Ferroelectrics*, **32**, 17 (1981).
14. S. Tasaka and S. Miyata, "Contemporary Topics in Polymer Science," Vol. 4, Plenum Press, New York, 1983, p 233.
15. S. Tasaka, K. Shiraishi, K. Murakami, and S. Miyata, *Sen-i Gakkaishi*, **39**, 456 (1983).
16. R. G. Kepler and R. A. Anderson, *J. Appl. Phys.*, **49**, 1232 (1978).
17. S. Tasaka and S. Miyata, *Kobunshi Ronbunshu*, **36**, 689 (1979).